



140
436
THS

1
2007



This is to certify that the
thesis entitled

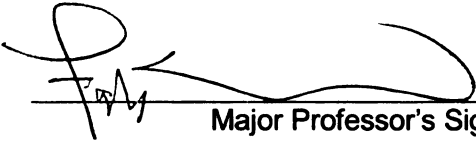
**A WIRELESSLY CONTROLLED MAGNETIC FORCE
ACTUATOR AND ITS AFM MEASUREMENTS**

presented by

Faisal T. Abu-Nimeh

has been accepted towards fulfillment
of the requirements for the

M.S. degree in Electrical and Computer Engineering


Major Professor's Signature

May 23, 2007
Date

PLACE IN RETURN BOX to remove this checkout from your record.
TO AVOID FINES return on or before date due.
MAY BE RECALLED with earlier due date if requested.

DATE DUE	DATE DUE	DATE DUE

**A WIRELESSLY CONTROLLED MAGNETIC FORCE
ACTUATOR AND ITS AFM MEASUREMENTS**

By

Faisal T. Abu-Nimeh

A THESIS

Submitted to
Michigan State University
in partial fulfillment of the requirements
for the degree of

MASTER OF SCIENCE

Department of Electrical and Computer Engineering

2007

ABSTRACT

A WIRELESSLY CONTROLLED MAGNETIC FORCE ACTUATOR AND ITS AFM MEASUREMENTS

By

Faisal T. Abu-Nimeh

Nanotechnology enables imaging and manipulating objects at the nanoscale possible. However, the majority of instruments and tools used in Nanotechnology include bulky equipment and require large voltages. In particular, actuation is typically achieved via Piezo material that requires voltages over the hundred volt range. The present thesis describes a portable low-power (low-voltage) magnetic force actuator module controlled wirelessly using the Zigbee protocol and its Atomic Force Microscopy (AFM) measurements. The contribution of the study is three fold: first, we design, simulate, and test a chip, which produces eight different magnetic force levels using the AMI $\mu 0.5m$ CMOS technology. All circuit components are implemented on the same die by minimizing their sizes and also minimizing the number of I/O pins. Thus, the circuit design real-estate size is $535\mu m \times 378\mu m$. Second, we implement an embedded software to wirelessly control the actuator chip via the Zigbee protocol. The software implements two command methods; either an automated command by executing a preprogrammed algorithm stored on a microcontroller, or a manual command by processing the user's input during runtime. Third, we measure the nano-Newton electromagnetic (EM) forces generated using the AFM by placing a magnetically doped cantilever (MFM: Magnetic Force Mode) over of the actuator platform and monitor its deflection for different force generated (EM) levels.

To my parents.

ACKNOWLEDGMENTS

First, I would like to thank my family for their great support and guidance. Despite the great distance between us they have always been there for me throughout my educational journey.

I would like to thank Professor Fathi Salem for his kind efforts and help since the beginning of my graduate studies. I have learned a lot during my work in his lab. His vast experience and enlightening advice made this thesis work possible. Also, many thanks to Professor Shantanu Chakrabartty and Professor Subir Biswas for their assistance and help throughout my studies.

Finally, thanks to all faculty, staff, and students at Michigan State University specifically those in the Electrical Engineering Department for making this a great institution and learning environment.

TABLE OF CONTENTS

LIST OF TABLES	vii
LIST OF FIGURES	viii
1 Introduction	1
1.1 Background and Motivation	1
1.2 Design Specifications	2
1.3 Thesis Organization	3
2 CMOS Magnetic Force Actuator	5
2.1 Introduction	5
2.2 Digitally Controlled Class E Power Amplifier	5
2.2.1 Introduction	5
2.2.2 Class E Power Amplifier	6
2.2.3 Digitally Controlled Switches	12
2.2.4 Thermometer Decoder	14
2.2.5 Magnetic Force Actuator	17
2.3 Conclusion	21
3 Wireless Control	23
3.1 Introduction	23
3.2 Zigbee Protocol	24
3.2.1 Introduction	24
3.2.2 Zigbee devices	24
3.2.3 Zigbee Stack	27
3.3 Wireless Nodes	28
3.3.1 Controller (Coordinator)	28
3.3.2 End Devices (MFA Nodes)	31
3.4 Conclusion	33
4 Atomic Force Microscope	34
4.1 Introduction	34
4.2 Magnetic Force Measurements	36
4.2.1 Introduction	36
4.2.2 Measurements	36
4.2.3 Conclusion	40

5	Conclusions	43
5.1	Results	43
5.2	Future Work	46
APPENDICES		47
A	Magnetic Force Actuator Test Chip	47
BIBLIOGRAPHY		50

LIST OF TABLES

2.1	Simulation Results for Output Power with Different Inputs.	14
2.2	Thermometer Decoder INPUT/OUTPUT	15
3.1	Zigbee Operational Frequency, Bit Rate, and Number Of Channels .	24
3.2	Manual User Input Using Switches	30
4.1	Comparison Between AFM and Other Technologies	36
4.2	Different User Inputs with their Corresponding Deflections	39
4.3	Different User Inputs with their Corresponding Forces	40

LIST OF FIGURES

2.1	Class E Power Amplifier	6
2.2	Optimum waveforms for maximum efficiency[1]	8
2.3	60nH Spiral Inductor	9
2.4	Class E PA when M1 is ON	9
2.5	30nH Spiral Inductor	10
2.6	Class E PA when M1 is OFF	10
2.7	1pF poly-poly2 Capacitor	12
2.8	8-bit Digitally Controlled Class E PA	13
2.9	Output Power 8-bit Digitally Controlled Class E PA	14
2.10	VHDL Code for Thermometer Decoder 3-to-8	16
2.11	3-to-8 Thermometer Decoder Schematic	16
2.12	A 6 micron by 6 micron Actuator	17
2.13	Unstacked Metal Layers for The Actuator	17
2.14	3D Angle View for The Magnetic Force Actuator	18
2.15	3D Side View for The Magnetic Force Actuator	18
2.16	AMI 0.5 Metals and VIA Properties	19
2.17	Current Passing Through The 20pH Inductor	20
2.18	Final Schematic for The Magnetic Force Actuator	21
2.19	Final Layout for The Magnetic Force Actuator	22
3.1	Magnetic Force Actuator in A Star Network Configuration	25
3.2	Zigbee Protocol Stack Architecture [2]	27
3.3	Coordinator Interrupt Routine to Start Actuation	29
3.4	Coordinator User Input Manual Actuation	30
3.5	Coordinator Preprogrammed Auto Actuation	31
3.6	RFD Node Receiving 3-Bits That Represent 8 Levels	32

4.1	Atomic Force Microscope [3]	35
4.2	Tip Deflection at 111	38
4.3	Tip Deflection at 110	39
4.4	Tip Deflection at All Input Levels	40
4.5	Force Exerted On Tip at All Input Levels At Distance Z1	41
4.6	Magnetic Cantilever on Top Of MFA	42
5.1	Magnetic Force Actuator Chip	43
5.2	Force Exerted On Tip at All Input Levels At Distance Z1	44
5.3	Magnetic Cantilever on Top Of MFA	44
5.4	Thesis Block Diagram	45
A.1	MFA Test Chip Layout	47
A.2	MFA Fabricated Test Chip	48
A.3	MFA Pin Diagram	49

CHAPTER 1

Introduction

This chapter provides a brief introduction of the overall thesis, starting with the background and motivation, then going over the design challenges and specifications, and finally ending up with the organization of this thesis.

1.1 Background and Motivation

As engineers, we are instructed and taught how to design things, however, any design by itself has different levels. Starting at the bottom: the device level is considered the lowest[4] then the circuit, gate, module, system, and all the way up to the application level. This work involves many levels of design. It starts with the device level to build up a system that is fabricated on a chip, which is later used with other components to deliver a final design. The three major components of this design are:

- A fabricated chip that contains a magnetic force actuator.
- Programmed wireless nodes to communicate with the chip mentioned above.
- An Atomic force microscope (AFM) to sense and measure the actuated force.

The thesis work integrates these components into a working system and executes experiments to demonstrate the system's functionality.

The on-chip actuator generates eight different levels of electromagnetic forces in the nano ranges suitable for nanotechnology applications and it uses low voltage power supplies (5 volts for the AMI $0.5\mu m$), in contrast with Piezo material based nano-positioning actuators which require very high voltages (100+ volts) [5]. Therefore, the proposed low voltage actuator can be portable and thus wireless command and control becomes an option. On the other hand, several applications require precise positioning, thus demand nano accuracy for their forces. For example, in lithography and semi-conductor fabrication processing, precise incremental forces are required. In [6] a motor-piezo technique is used for nano scale precision but that requires extra elements to compensate for nonlinearities and hysteresis. Whereas in this work, an integrated 8-bit digital input provides incremental and stable eight different levels of actuation to provide the desired forced. Consequently, the size of the actuator, the way it is controlled, the low power requirements, and incremental digital actuation make the proposed work more attractive for nano applications.

Measuring and validating the nano-Newton level forces becomes a challenge for present day measuring devices. In this work, an AFM is used to quantify the CMOS silicon generated force for accuracy and resolution.

1.2 Design Specifications

Each component mentioned in the previous section has its own specification. Starting with the fabricated chip, its design requirements are:

- The size of the chip (area) has to be as small as possible.
- An easy interface to control the chip with near linear behavior.
- All components have to be integrated on one die.
- The power consumed by the chip has to be as minimum as possible.

The second part of this work deals with programming wireless nodes to communicate with the chip and it is required to have the following specifications:

- Two or more wireless nodes are for communication and/or control.
- The size of the code should be minimal.
- The algorithm used to control the chip is computed and executed remotely.
- The wireless nodes should not consume much power.

The last part, which is the AFM, is required to have the following specifications:

- The ability to measure small magnetic forces.
- The cantilever tip should be small enough to access the small elements on the fabricated chip.

These were the overall specifications for this work. An in-depth assessment will be discussed for each requirement in its corresponding chapter to explain why and how such requirements were attained.

1.3 Thesis Organization

The first chapter includes a brief introduction of the project. It contains three sections, the first one is background and motivation, the second one lists the design specifications, and the third one describes the organization of this thesis.

Chapter two included all material regarding the fabricated chip with detailed specifications, simulations, and experimental results.

Chapter three describes how the fabricated chip can be controlled wirelessly using the Zigbee protocol with examples and real implementations.

Chapter four introduces the AFM module and how it is utilized it to measure the output of the fabricated chip.

Finally, the last chapter gives an overview of the entire system with all components and possible future work.

CHAPTER 2

CMOS Magnetic Force Actuator

2.1 Introduction

This chapter discusses the design process and results for the fabricated CMOS chip that contains a Class E power amplifier, a Thermometer Decoder, and a Magnetic Field Actuator. Each component will be explained separately and in the last section a summary of the whole chip will be given. The current CMOS technology used for this project is the AMI C5N n-well 0.5μ and 0.30λ technology [7] which features 3 metal layers, 2 poly layers, and a high resistance layer. The supply voltage used with this technology is 5 volts, consequently all circuits will be designed and optimized for 5V.

2.2 Digitally Controlled Class E Power Amplifier

2.2.1 Introduction

Power Amplifiers (PA's) are one of most important elements in a CMOS transceiver. Its power consumption is significant to the overall total power used. Thus, making it as efficient as possible yields great savings specially for low power applications. Achieving high efficiency in CMOS is limited by low breakdown voltage, low current drives, substrate noise, etc. However, there are techniques to go around them.

Another important requirement is linearity, which makes the usage, design, and operation easier. The PA included in this work is similar to that designed in [8], however, with few minor changes it can be exploited for different applications.

2.2.2 Class E Power Amplifier

The first generation of the nonlinear Class E PA appeared in the mid 70's when Sokal[1] introduced a highly efficient PA with a 100% ideal efficiency. The Class E amplifier relies on the fact that the active device, FET or BJT, operates as a switch instead of current source. It became very attractive due to its simple design and robust behavior. Figure 2.1 is a simple Class E PA and it contains three major elements: the transistor M1 which acts as a switch, a filter (C_2, L_2) which tunes the output to a certain frequency, and a RFC (Radio Frequency Choke) large inductor that assures that the peak to peak swing at the output load is close to $3.6 \times V_{DD}$ and acts as a DC current source[9].

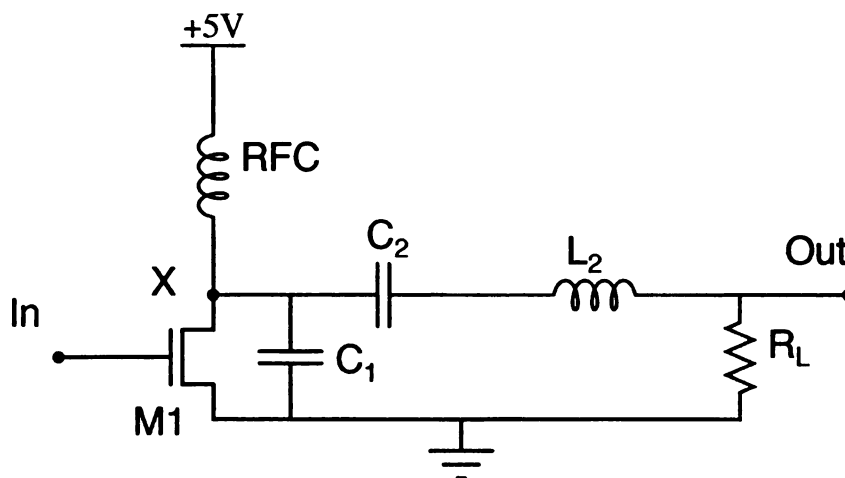


Figure 2.1. Class E Power Amplifier

M1 operating as an ideal switch, meaning that there is no overlapping period of nonzero switch voltage and current. So, when the switch is ON, the drain voltage at X is zero and when the switch is OFF, the current flowing into M1 is zero. Figure

2.2 shows the ideal wave form for the switch M1 where the current and the voltage do not intersect at the same time. However, the transition between the ON and OFF state has a finite time, so, that's when losing power occurs. To eliminate this an abrupt transition between the ON and OFF state is desired. However, in reality this does not exist, consequently a step function input is used with very small rise/fall time. Also, for none ideal conditions a shunt capacitor C1 is used to reduce the switching losses that occur during the transition from ON to OFF to make sure that the voltage at X increases from zero just after the current stops flowing into M1. On the other hand, the inductor L2 and the capacitor C2 can also minimize the losses during the transition from OFF to ON by assuring that voltage goes to zero just before the switch current increases. The criterion for selecting the shunt capacitor C1 is: neither too large to be considered a harmonic short nor too small to become a device parasitic[10].

The methodology used to design such a PA is straight forward. Starting with the RFC: inductor, it should provide a DC path from the supply and is approximately an open circuit at RF[11]. Hence, it has to be large enough to provide enough current, consequently, a 60nH on-chip spiral inductor was designed and it is shown in figure 2.3. The dimensions of the spiral are $103\mu\text{m}$ by $103\mu\text{m}$, the width of the metal layers is $1.8\mu\text{m}$, the spacing between metals is $0.9\mu\text{m}$, the number of turns (windings) is 18, and finally the metal layers used are Metal3 and Metal2 (exit). Note that the size, spacing, and width is as minimal as possible to make sure that we can implement the smallest functional chip possible using the AMI 0.5μ technology. Even though we have a 1.5mm by 1.5mm real-estate but keeping the overall used area minimal is crucial for certain future applications. This inductor was designed using ASITIC[12], using the command in (2.1). The resulting spiral inductor had an inductance approximately equals to 60nH and a Q value of 1.2.

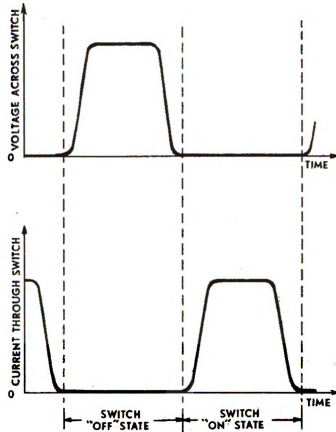


Figure 2.2. Optimum waveforms for maximum efficiency[1]

$$sqmmname = ind60 : len = 103 : w = 1.8 : s = 0.9 : n = 18 : metal = m3 : exit = m2 \quad (2.1)$$

The next part is to tune the PA to run at the desired frequency 900MHz. To achieve that high frequency two on chip passive elements were designed; a 45.5 pF capacitor and a 30nH inductor. Therefore, two models characterize this Class E PA: when the switch is turned ON and the other one is when the switch is turned OFF.

First, when the switch is ON, figure 2.4 shows the model consisting of a simple RLC. This part can be clearly used as a band pass to block other frequencies and to minimize the harmonic distortion caused by other elements[13]. This model will produce a resonance frequency based on equation (2.2) where ω_o is the operational

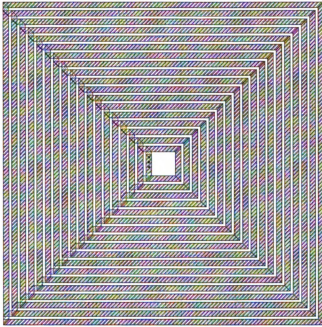


Figure 2.3. 60nH Spiral Inductor

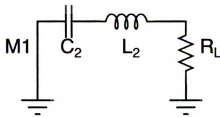


Figure 2.4. Class E PA when M1 is ON

frequency.

$$\omega_o = \frac{1}{\sqrt{C_2 \cdot L_2}} \quad (2.2)$$

To stay within constrains of the technology and real-estate limitations we chose L_2 to be 30nH. Again, ASITIC was used to simulate and design this spiral inductor as shown in figure 2.5. The dimensions of the spiral are $103\mu\text{m}$ by $103\mu\text{m}$, the width of the metal layers is $1.8\mu\text{m}$, the spacing between metals is $1.8\mu\text{m}$, the number of turns (windings) is 10, and finally the metal layers used are Metal3 and Metal2 (exit). The only difference between the 30nH inductor and the 60nH is the spacing used between

the metals and the number of turns. By plugging in $L_2 = 30\text{nH}$ and $\omega_o = 900\text{MHz}$ in equation (2.2) then C_2 will be 45.5pF .

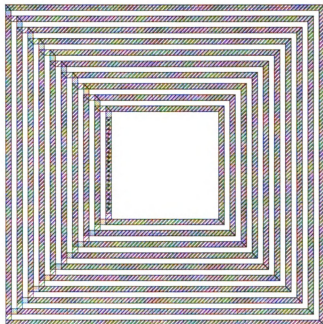


Figure 2.5. 30nH Spiral Inductor

Alternatively, when the switch is OFF the circuit can be represented as shown in figure 2.6.

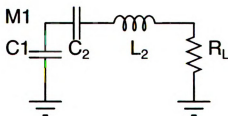


Figure 2.6. Class E PA when M1 is OFF

Using the same values for L_2 and C_2 from the previous model we find C_1 to be 41.5pF using (2.3).

$$\omega_1 = \frac{1}{\sqrt{L_2(C_2 \cdot C_1) / (C_2 + C_1)}} \quad (2.3)$$

However, this value will reduce the efficiency of the circuit. Because when the switch is OFF the big inductor RFC in figure 2.1 will start filling up the Capacitor C_1 . So, by the time the switch is back on, C_1 has to get rid of all the charge it has stored and if it doesn't then the charge will be wasted by the switch and that will reduce the efficiency of the PA. Therefore, the optimal C_1 should be calculated[14] using equation (2.4).

$$C_1 = \frac{P_{out}}{\pi\omega V_{DD}^2} \quad (2.4)$$

where P_{out} is the power at the output, ω is the operational frequency, and V_{DD} is the power supply voltage. Assuming that the PA is connected to a 50Ω load, the power at the output can be estimated with equation (2.5).

$$P_{out} = \frac{8V_{DD}^2}{R(\pi^2 + 4)} \quad (2.5)$$

By substituting P_{out} in equation (2.4) with (2.5), C_1 will be approximately 1pF. Both capacitors C_1 and C_2 has been designed using two consecutive conducting plates of polysilicon. Using the values from the previous MOSIS runs for AMI 0.5μ the capacitance between the two layers poly and poly-2 equals $c(\text{poly-poly2}) = 0.914\text{fF}/\mu\text{m}^2$. To find the size of the capacitor we need to calculate the ratio (S) between the desired capacitance and the sheet unit capacitance. Therefore, $S = \frac{\text{DesiredCapacitance}}{\text{SheetCapacitance}}$ so, $S = \frac{45.5\text{pF}}{0.914\text{fF}} = 45.405k$, so, the length and the width (because it is a square) is $213\mu\text{m}$ (to the nearest λ). The same calculation is carried out for the 1pF capacitor and it yields a length which equals $33.15\mu\text{m}$, shown in figure 2.7.

All the parameters needed for the PA are ready except for the switching part which will be discussed in the next subsection. To summarize the values, The RFC inductor is 60nH, shunt capacitor C_1 is 1pF, to tune the output frequency a bandpass filter with C_2 equals to 45.5pF and L_2 30nH, and finally the load R_L is considered to be a 50Ω load.

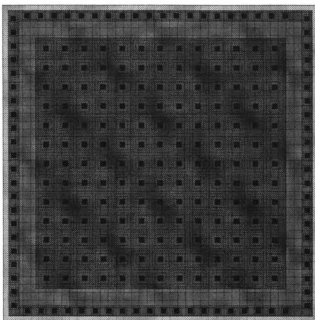


Figure 2.7. 1pF poly-poly2 Capacitor

2.2.3 Digitally Controlled Switches

From the previous subsection as shown in figure 2.1 the switch M1 is a simple NMOS transistor. Therefore, when we consider the technology we are using, it is important to operate the switch as fast as possible to accommodate the 900MHz input frequency. So, to match this requirement, the size of the transistor M1 has to be as small as possible. Additionally, to increase the power of the PA [15] the transistor M1 can be replaced with a parallel configuration of NMOS transistors (M1,...,M8). This configuration also uses the minimum size allowed W/L ratio to cope with the 900MHz input frequency.

The eight transistors added to the PA could allow more current to be delivered to the output, however, adding more transistors to the parallel configuration will not result in a significant change in the current delivered, because the circuit actually saturates and it can no longer deliver more current to the output.

Having eight transistors as inputs allows us to have eight different power output

levels by switching transistors ON/OFF when needed. Therefore, an AND gate is used to allow the user to control the power at the output. Figure 2.8 shows the overall PA circuit where the external DCO (digitally controlled Oscillator) can be replaced with a VCO (Voltage Controlled Oscillator) running at 900MHz [15]. The user inputs (Input1 thru Input8) will decide which transistors should be ON/OFF. When all transistors are ON, the PA delivers its most power, and when all transistors are OFF, the PA should be turned off. Therefore to do this simple selection with the DCO and the AND gate designed is just a simple static CMOS AND gate.

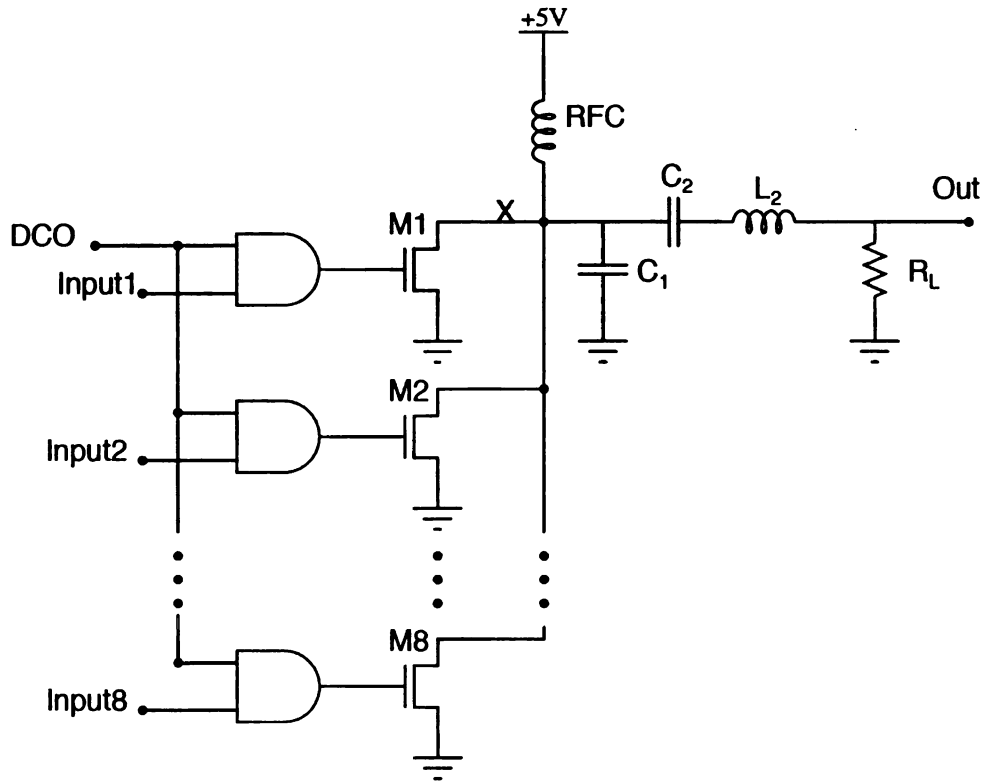


Figure 2.8. 8-bit Digitally Controlled Class E PA

Figure 2.8 was simulated with 8 different input levels using Cadence Virtuoso to study the power at the output. Table 2.1 shows the results of these simulations. Each simulation was conducted by itself. However, as the number of ON transistors increases the contribution to the overall power of the new transistor added decreases, which explains/proves that the circuit is actually nearing saturation. This can be

Table 2.1. Simulation Results for Output Power with Different Inputs.

Number of ON Transistors	Output Power (dbm)
0	-16.3
1	-12.3
2	-9.01
3	-7.25
4	-6.01
5	-5.04
6	-4.25
7	-3.58
8	-3

clearly seen in figure 2.9.

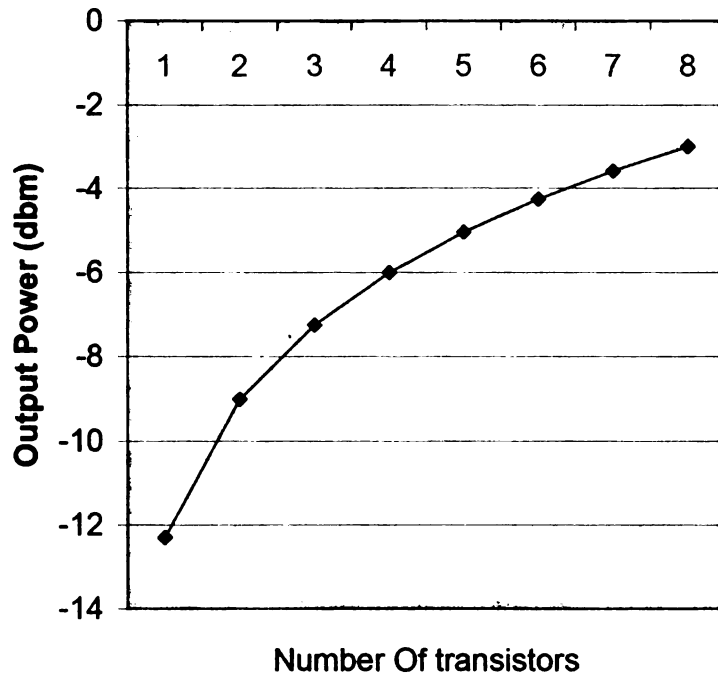


Figure 2.9. Output Power 8-bit Digitally Controlled Class E PA

2.2.4 Thermometer Decoder

To keep the size as minimal as possible and to keep the number of pins on the chip as minimal as possible, a 3 to 8 decoder is implemented. The way this decoder operates is different than the known standard decoders because we don't just want to send the PA one bit at a time. The reason behind that is the way the PA functions; when one

Table 2.2. Thermometer Decoder INPUT/OUTPUT

3-Bit Input	8-Bit Output
000	00000001
001	00000011
010	00000111
011	00001111
100	00011111
101	00111111
110	01111111
111	11111111

transistor is ON that gives us one power level when two transistors are ON that gives us two power levels. Therefore, we need a decoder which sends more than one bit at a time to cause the PA to turn on more than one transistor simultaneously. So, the best choice would be a thermometer decoder which can be summarized in table 2.2. At any point there is at least one transistor switched ON. This guarantees that the number of ON switches can be controlled precisely because there is no overlap. In addition, because of the fact that the transistors are connected in parallel, the location of the ON switch does not really matter so the order of bits in the Thermometer Decoder is not crucial.

The design of this decoder was accomplished using VHDL and Cadence Silicon Ensemble and it was optimized to use the minimal real-estate possible on the chip. Figure 2.10 shows the VHDL code for this decoder.

The schematic generated using this VHDL code contains 9 gates as illustrated in figure 2.11. The overall area of the decoder is about $73\mu m^2$. The standard cell used to generate this decoder is OSU Standard Cell Library v2.1[16] along with NCSU CDK v1.5.1[17].

```

library IEEE;
use IEEE.std_logic_1164.all;
use IEEE.std_logic_unsigned.all;

entity LOGC3T08 is
  port (SEL: in STD_LOGIC_VECTOR(2 downto 0);
        LOGC_OUT: out STD_LOGIC_VECTOR(7 downto 0));
end LOGC3T08;

architecture BEHAV of LOGC3T08 is
begin
  WITH SEL SELECT LOGC_OUT <=
    "11111111" WHEN "111",
    "11111110" WHEN "110",
    "11111100" WHEN "101",
    "11111100" WHEN "100",
    "11111000" WHEN "100",
    "11110000" WHEN "011",
    "11100000" WHEN "010",
    "11000000" WHEN "000",
    "10000000" WHEN OTHERS;
end BEHAV;

```

Figure 2.10. VHDL Code for Thermometer Decoder 3-to-8

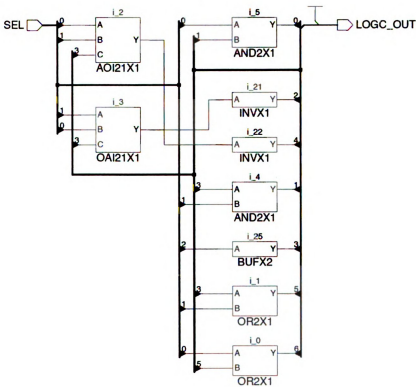


Figure 2.11. 3-to-8 Thermometer Decoder Schematic

2.2.5 Magnetic Force Actuator

The magnetic force actuator is simply a spiral inductor replacing the R_L load in the Class E PA described in the previous section. The design criterion for the magnetic force actuator is creating a three metal layer inductor with the smallest dimensions possible. This resulted in a $6 \times 6 \mu\text{m}^2$ square with three layers as shown in figure 2.12. The windings of the spiral inductor for each layer is not a full square, one of the sides is missing so that makes a three quarter square or a square with three sides. Again, the inductor was designed using ASITIC and its inductance came out to be 20pH.



Figure 2.12. A 6 micron by 6 micron Actuator

If we unstack the metal layers in figure 2.12. The shape of the metal layers would look like figure 2.13. Note, that Metal3 is on the left, Metal2 is in the middle, and Metal1 is on the right. The access pin of this actuator is located on the upper right corner of Metal3 layer and the exit pin is located on the upper left corner of Metal1. The layers are connected using the smallest sized VIA1 and VIA2.

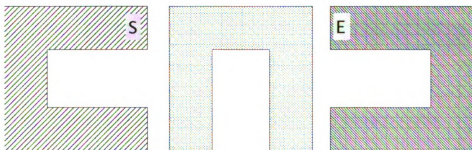


Figure 2.13. Unstacked Metal Layers for The Actuator

The actuator can be approximated with a Solenoid, consequently, when a current

passes through it the actuator can generate a uniform magnetic field similar to the one generated by a bar magnet. However, the direction of the magnetic field will be alternating because the output of the PA is AC. The 3D structure of the actuator along with the direction of the current is previewed in figures 2.14 and 2.15.

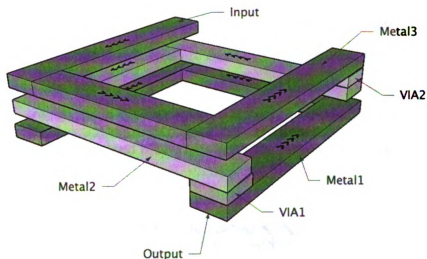


Figure 2.14. 3D Angle View for The Magnetic Force Actuator

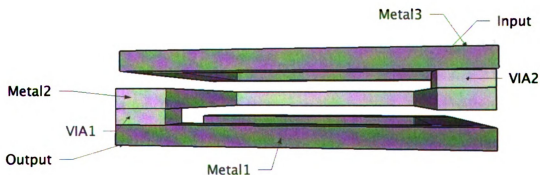


Figure 2.15. 3D Side View for The Magnetic Force Actuator

The Class E PA will have the inductor shown in figure 2.14 as a load. So, all of the current going into the load will be actually going through it, therefore, it will generate a magnetic force coming out of in the center of the inductor depending on

the direction of the current. The magnetic field can be approximated as in equation (2.6)[18]

$$B = \mu_{SiO_2} \frac{N}{L} I \quad (2.6)$$

where B is the magnetic field, μ permeability, N is the number of turns, L is the length (in our case, the length is in the Z direction), and I is the current. The X and Y dimensions of the spiral inductor are $6\mu m$ by $6\mu m$ however, the Z is not known. The technology file model used to design this spiral inductor in ASITIC states that the thickness of Metal1 is $0.5\mu m$, Metal2 is $0.5\mu m$, and Metal3 is $0.8\mu m$. The distance between M1/M2 is $0.5\mu m$, and M2/M3 is $0.5\mu m$ as shown in figure 2.16, therefore, The unknown Z is $2.8\mu m$.

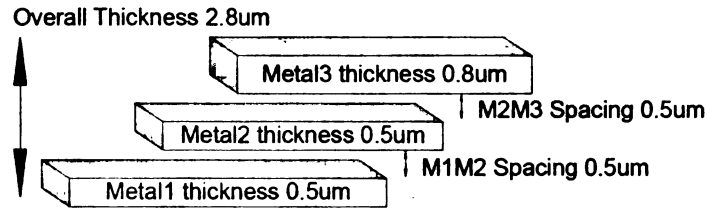


Figure 2.16. AMI 0.5 Metals and VIA Properties

Also, $\mu_{SiO_2} = 1/c^2 \epsilon_{SiO_2}$ = the reciprocal of the speed of light squared times the permittivity of SiO_2 , which equals to 3.18×10^{-7} . Now $N = 3$ turns, $L = 2.8\mu m$, and $I = i(t)$ and it is a function of time as seen in figure 2.17. The Frequency of the waveform is 900MHz. Thus, the magnetic field will be alternating and will have two different directions per cycle. The maximum field generated is exactly at peaks of the current function which are located at $\frac{1}{4}$ and $\frac{3}{4}$ of the period where the magnitude is approximately $|8|mA$. This will give us a rough estimate of B which equals to 2.724×10^{-3} Tesla. However, to get a better magnetic field off the chip we designated an “UNPASSIVATED DIE” with a glass cut on top of the actuator (20pH inductor).

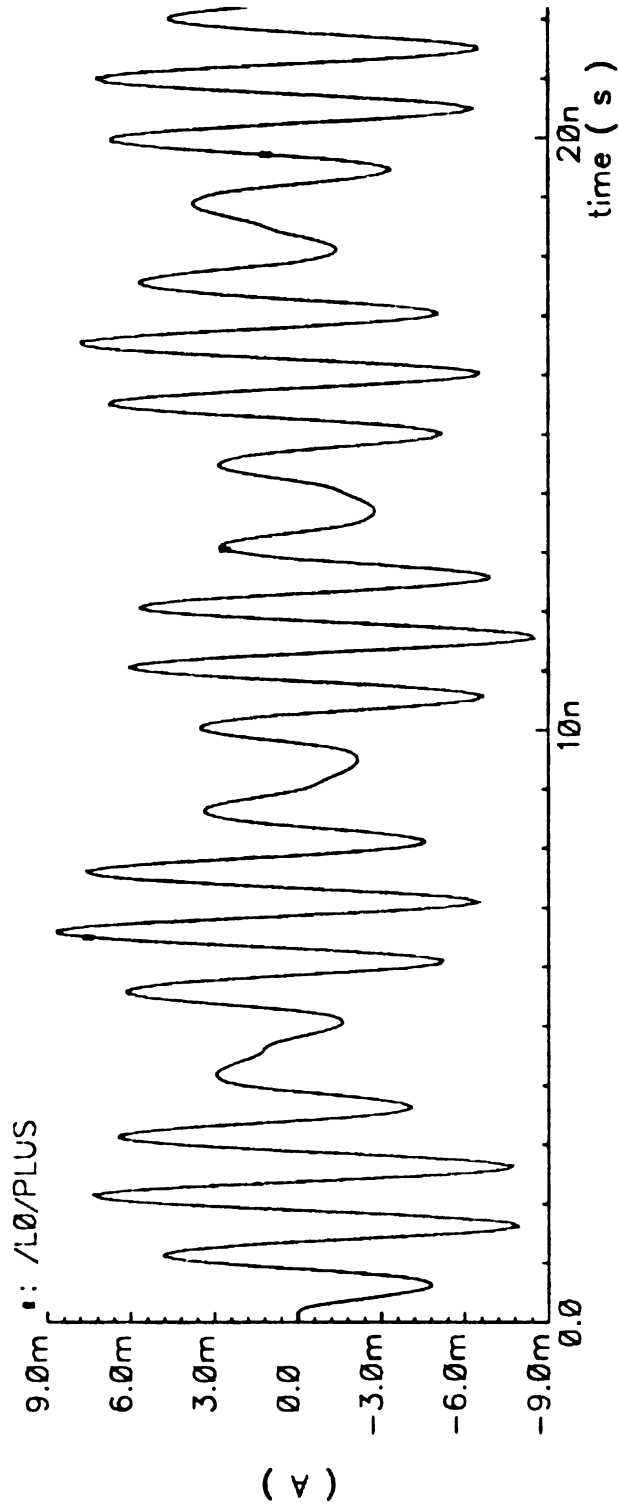


Figure 2.17. Current Passing Through The 20pH Inductor

2.3 Conclusion

An on-chip digitally controlled Class E Power Amplifier with an on-chip spiral inductor connected as load to actuate magnetic force is designed, simulated, and fabricated using the AMI $0.5\mu m$ technology. Figure 2.18 illustrates the final schematic of the final circuit.

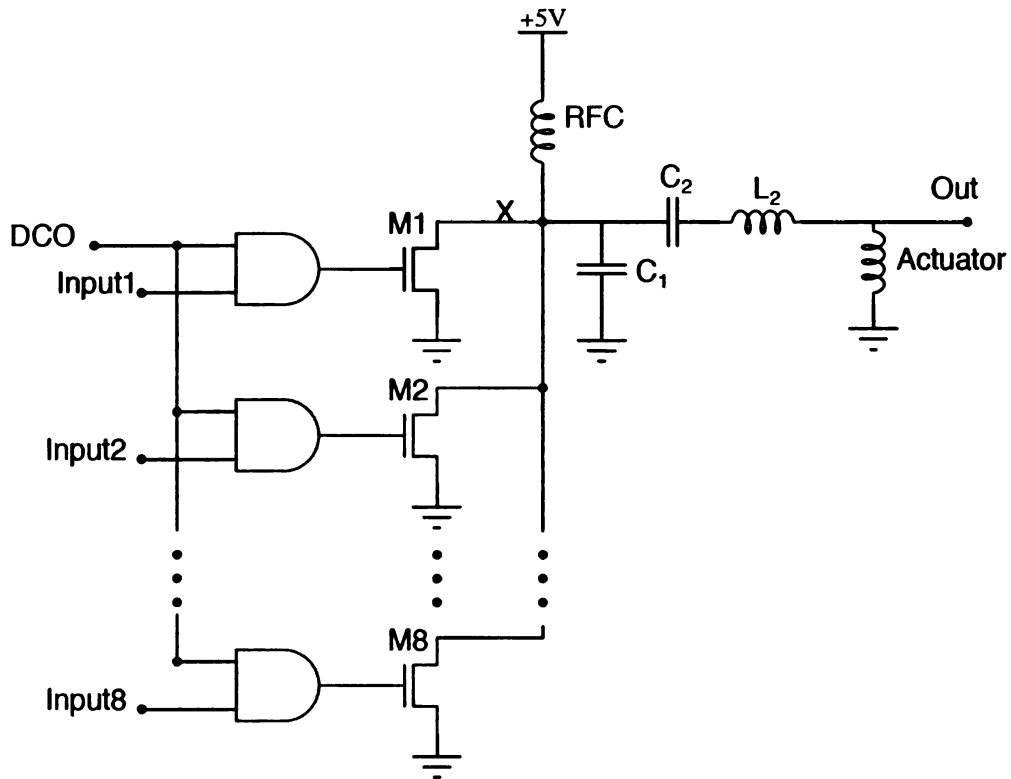


Figure 2.18. Final Schematic for The Magnetic Force Actuator

The pad frame area is $1.5\text{mm} \times 1.5\text{mm}$, the actuator with all components consumed $535\mu m \times 378\mu m$ area as shown in figure 2.19, so other three PAs were placed for test purposes. The full layout has been included in Appendix A.

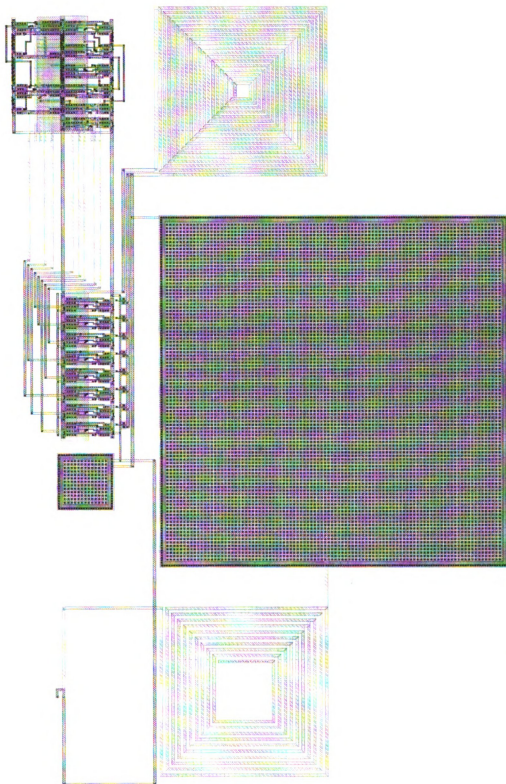


Figure 2.19. Final Layout for The Magnetic Force Actuator

CHAPTER 3

Wireless Control

3.1 Introduction

This chapter covers the requirements, design, and results for the Wireless Control. As discussed in the previous chapter, an 8-bit digitally controlled magnetic force actuator was designed and fabricated, so, to utilize its small design and low power properties, we used the Zigbee protocol to interface and control it wirelessly. Because Zigbee was designed for low data rate, low power, and reduced resource requirements we chose it over other protocols. The main goal is to create an arbitrary number of magnetic force actuators to form a wireless sensor network. A single Coordinator (Controller) will operate the sensor network with two methods: It can either send commands based on a preprogrammed control algorithm or it can send commands using a manual user input. The controlling commands are actually a 3-bit representation of the desired magnetic force to be generated. The Microchip Zigbee ICDEM Z kit was adopted to provide a platform for this wireless control.

3.2 Zigbee Protocol

3.2.1 Introduction

The Zigbee Protocol follows the IEEE 802.15.4 specifications for its Medium Access Layer and Physical Layer. It uses the ISM radio bands; 868MHz, 915MHz, and 2.4GHz. For each band there exists a fixed number of channels to operate on. The bit rate is variable and it depends on the operational frequency. 868MHz can provide up to 20kbps, 915MHz up to 40kbps, and finally 2.4GHz up to 250kbps [19]. These numbers are summarized in table 3.1.

Table 3.1. Zigbee Operational Frequency, Bit Rate, and Number Of Channels

Frequency	Bit Rate	Channels
868MHz	20kbps	1
915MHz	40kbps	10
2.4GHz	250kbps	16

3.2.2 Zigbee devices

The IEEE 802.15.4 specifies two types of devices: FFD(Full Function Device) and RFD (Reduced Function Device). The main difference between these two devices is the power. For an FFD device it is assumed that it can offer all kinds of services while the RFD can only support limited services. Also, because the FFD has to support everything it must stay “awake” all the time and this requires a constant reliable power source. On the other hand, the RFD will “sleep” when it is idle, therefore, it will run on batteries or other low power sources.

The Zigbee protocol emphasizes these types differently depending on the application. There are three device types stated in the Zigbee Protocol:

- Coordinator: Modeled as a FFD. It forms the network, allocates addresses, and keeps the binding table.

- Router: Modeled as a FFD. It extends the range and capacity of the network and can have monitor or control functionality.
- End Device: Modeled as a RFD (or even FFD). It has monitoring or controlling functions.

In this work, the magnetic force actuator chips are considered as “End Devices” and they operate as Reduced Function Devices to utilize their low power properties. The actuators will not communicate with or control each other because that job is assigned to the Coordinator (FFD) only. This even reduces the RFD requirements further. Therefore, the network architecture used for this work is “Start Network Configuration” where there exists only one Coordinator and several End Device nodes (magnetic force actuators) as illustrated in figure 3.1. There are several other configurations available in the Zigbee Protocol like “Cluster Tree Topology” and “Mesh Network”. By using the simplest model possible, we guarantee that the software implementation remains as minimal as possible, which reduces the overall overhead and required microprocessing resources.

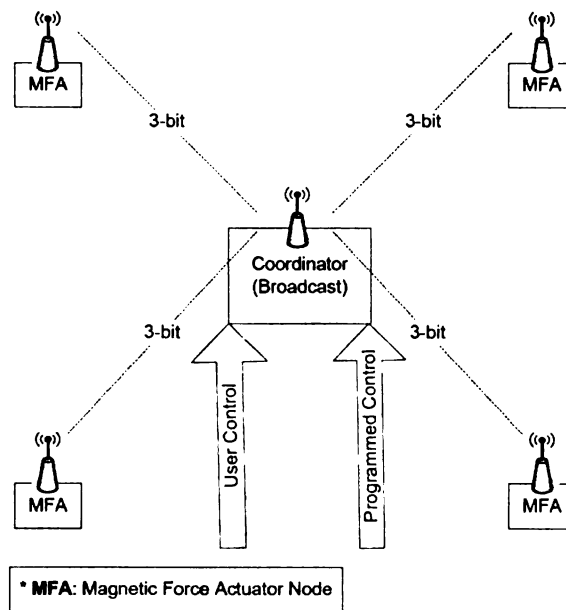


Figure 3.1. Magnetic Force Actuator in A Star Network Configuration

Each node (FFD or RFD) has two addresses: a 16-bit network address which is acquired once a node successfully joins a network and this address will be used to communicate with the coordinator. The second address is a 64-bit MAC address which is hardcoded and it has to be globally unique. This is analogous to IP (Internet Protocol), where each device has an IP address and a MAC address, The MAC address is hardcoded on the ethernet device for example while the IP address is obtained once the device joins/forms a network.

The Zigbee protocol uses the IEEE 802.15.4 MAC which is 127 bytes long and it contains a 16-bit CRC value for error checking. It can also contain ACK flags for data transfer acknowledgment. A packet with an ACK flag requires the targeted node to confirm the reception of that packet, however, that only assures receptions but not complete processing. A node might receive a packet but might not process it due to some limitations. Therefore, this kind of confirmation should be implemented in the application layer. it is important to know that, with the ACK flag the sender will retransmit the packet for a fixed number of tries then report failure.

The Coordinator can send packets to a specific (MFA) Magnetic Force Actuator Node by providing its 16-bit destination address in the MAC layer header. This method is called Unicast and it is not currently used but it can be easily enabled to expand the functionality further. On the other hand, Broadcasting is used in this work, the destination address in the MAC layer is replaced with the broadcast address 0xFFFF. Any MFA will be able to receive these packets because Zigbee implements a passive acknowledgment feature where all broadcasting packets have to be rebroadcast again by all nodes and if one node does not rebroadcast other neighboring nodes will notice that it missed the broadcast packet and they will retransmit until the missing node hears it or time out occurs.

3.2.3 Zigbee Stack

A free implementation of the Zigbee protocol is provided by Microchip. Their Zigbee Stack v1.0-3.8 was used [2]. In this work, there are some limitations in this implementations. However, to control the Magnetic Force Actuator nodes wirelessly, none of these limitations affected us. Nevertheless, it provided extra functions which can be used later to expand the functionality of this wireless control. Figure 3.2 shows the Zigbee protocol stack architecture.

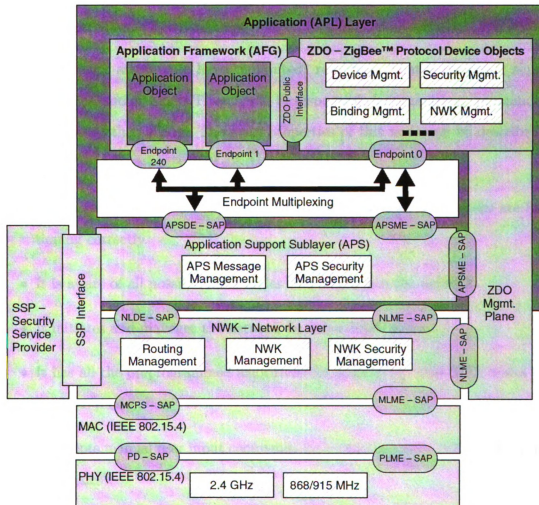


Figure 3.2. Zigbee Protocol Stack Architecture [2]

3.3 Wireless Nodes

As discussed in the previous section Zigbee provides two device models FFD and RFD. Each device has its own properties, thus, to take advantage of these properties and to make them fit with the requirements of this project the Controller (Coordinator) will be represented as an FFD and it will be responsible for forming the actuation network. On the other hand, the Magnetic Force Actuator nodes (MFAs) will be used as RFD devices and will only listen to commands broadcasted by the Controller.

3.3.1 Controller (Coordinator)

The Controller is assumed to have “unlimited” resources. That is the power supply, CPU resources, and memory. Thus, it will be responsible for organizing, commanding, and controlling other MFAs. The main properties of this node can be described as following:

- It remains awake all the time in order to assure that all MFA nodes are functioning correctly.
- It is aware of all possible MFA nodes that might join the network.
- It initiates and manages the network for other MFA nodes.
- It has all the preprogrammed algorithms for controlling other MFA nodes (automated mode).
- It accepts manual user input commands for controlling other MFA nodes (manual modes).

The Controller consists of four major parts: a microprocessor, 3 input switches, three push buttons, and a transceiver. First, The microprocessor used is an 8-bit PIC18LF4620 from Microchip. It processes user inputs (using interrupts shown in

figure 3.3), preprogrammed control algorithms, Zigbee stack, and interfacing with the transceiver and other components on the board. Second, the 3 input switches SW2, SW1, and SW0 are used as manual user input to control the MFA nodes, these switches are connected RD0, RD1, and RD2 on the microprocessor. The three switches represent the desired magnetic force actuated each switch triggers one bit, so, we have three bits and 2^3 possible numbers. Therefore, we can command the MFA nodes to produce eight different levels by using these switches as shown in table 3.2 and this is similar to what the Class E Amplifier had in table 2.2.

```

void UserInterruptHandler(void)
{
    // Is this an interrupt-on-change interrupt?
    #ifdef IMA_CONTROLLER
    if ( INTCONbits.RBIF == 1 )
    {
        // Record which button was pressed so the main() loop can
        // handle it

        if (AUTO_SWITCH == SWITCH_PRESSED)
        {
            myStatusFlags.bits.autoActuationStarted = TRUE;
            myStatusFlags.bits.autoActuationSwitch = TRUE;
            ConsolePutROMString( (ROM char *) "Start Automatic Actuation...\r\n" );
        }

        if (SEND_SWITCH == SWITCH_PRESSED)
        {
            myStatusFlags.bits.userInputSwitch = TRUE;
            ConsolePutROMString( (ROM char *) "Start User-Input Actuation...\r\n" );
        }
        // Disable further RBIF until we process it
        INTCONbits.RBIE = 0;

        // Clear mis-match condition and reset the interrupt flag
        LATB = PORTB;

        INTCONbits.RBIF = 0;
    }
    #endif
}

```

Figure 3.3. Coordinator Interrupt Routine to Start Actuation

Third, the three push buttons MCLR, S2, and S3 are used for initialization and triggering. The MCLR push button will reset the microprocessor to its initial state,

Table 3.2. Manual User Input Using Switches

SW2SW1SW0	Magnetic Force Actuated
000	<i>SmallestForce</i>
001	<i>Force1</i>
010	<i>Force2</i>
011	<i>Force3</i>
100	<i>Force4</i>
101	<i>Force5</i>
110	<i>Force6</i>
111	<i>LargestForce</i>

S2 is used to trigger the microprocessor to sample the inputs on SW0, SW1, and SW2 illustrated in figure 3.4 and then

```
if ( myStatusFlags.bits.userInputSwitch )
{
    myStatusFlags.bits.userInputSwitch = FALSE;
    ZigBeeBlockTx();

    TxBuffer[TxData++] = APL_FRAME_TYPE_KVP | 1; // KVP, 1 transaction
    TxBuffer[TxData++] = APLGetTransId();
    TxBuffer[TxData++] = APL_FRAME_COMMAND_SET | (APL_FRAME_DATA_TYPE_UINT8 << 4);
    TxBuffer[TxData++] = OnOffSRC_OnOff & 0xFF; // Attribute ID LSB
    TxBuffer[TxData++] = (OnOffSRC_OnOff >> 8) & 0xFF; // Attribute ID MSB

    SR_DATA = 0;
    SR_DATA = (USER_IO2 & 0x01);
    SR_DATA = SR_DATA << 1;
    SR_DATA = (SR_DATA & 0x02) | (USER_IO1 & 0x01);
    SR_DATA = SR_DATA << 1;
    SR_DATA = (SR_DATA & 0x06) | (USER_IO0 & 0x01);

    TxBuffer[TxData++] = SR_DATA;

    PrintChar( SR_DATA );
    ConsolePutROMString( (ROM char *)" SR_DATA being sent.\r\n" );
}
```

Figure 3.4. Coordinator User Input Manual Actuation

broadcast the resulting three bits to the MFA nodes, and finally the S3 push button triggers the microprocessor to start the automated mode were the preprogrammed algorithm will be executed and then broadcasted to the MFA nodes as shown in figure 3.5. The algorithm demonstrated in the figure is just a simple counter which will command each MFA node to actuate slowly from lowest force to highest then stop.

The fourth and last part is the transceiver. The Zigbee stack supports two transceivers Chipcon CC2420 and Microchip MRF24J40. In this work the Chipcon

```

if (myStatusFlags.bits.autoActuationSwitch)
{
    count++;
    myStatusFlags.bits.autoActuationSwitch = FALSE;
    ZigBeeBlockTx();

    TxBuffer[TxData++] = APL_FRAME_TYPE_KVP | 1;    // KVP, 1 transaction
    TxBuffer[TxData++] = APLGetTransId();
    TxBuffer[TxData++] = APL_FRAME_COMMAND_SET | (APL_FRAME_DATA_TYPE_UINT8 << 4);
    TxBuffer[TxData++] = OnOffSRC_OnOff & 0xFF;    // Attribute ID LSB
    TxBuffer[TxData++] = (OnOffSRC_OnOff >> 8) & 0xFF; // Attribute ID MSB

    SR_DATA = count-1;

    TxBuffer[TxData++] = SR_DATA;

    PrintChar( SR_DATA );
    ConsolePutROMString( (ROM char *)" SR_DATA being sent.\r\n" );
}

```

Figure 3.5. Coordinator Preprogrammed Auto Actuation

CC2420 transceiver is used and is controlled using the SPI interface. The Controller node will never switch off its transceiver and it will always book keep other nodes on the network.

3.3.2 End Devices (MFA Nodes)

The End Device is assumed to have “limited” resources. That is the power supply, CPU resources, and memory. Thus, its job is to listen/poll for certain commands from Controller then sleep to save power the main properties of these nodes are the following:

- It should sleep whenever it is idle.
- It is aware of other MFA nodes but it does not manage them.
- It does not try to perform its own network. It can only join pre-existing networks.
- There are no preprograms installed on it and its code remains as minimal as possible.

- It accepts broadcasted commands from the Controller only.

The major components of such nodes are: first the microprocessor where the Zigbee stack and minimal MFA functionality are stored, second, the transceiver similar to that described in the Coordinator. However, it must be noted that the current Zigbee stack is non-beacon which means that each MFA node should poll for data when it wakes up from sleep. There are three output pins on the microprocessor which are connected directly to the Magnetic Force Actuator Chip. Specifically, these three bits will be connected to the S2, S1, and S0 on the 3-8 thermometer decoder which will be later translated to different magnetic force using the Class E PA. For example, figure 3.6 shows when a data packet is received, it is processed in the RFD using a simple switch statement to figure out which one of the eight input levels was requested. The first three cases are shown below. It is also possible as previously discussed, to confirm with the Controller that this packet was successfully received.

```
switch (data)
{
    case DATA_ZERO:
        ConsolePutROMString( (ROM char *)" Received ZERO.\r\n" );
        USER_IO0 = 0;
        USER_IO1 = 0;
        USER_IO2 = 0;
        TxBuffer[TxData++] = SUCCESS;
        break;
    case DATA_ONE:
        ConsolePutROMString( (ROM char *)" Received ONE.\r\n" );
        USER_IO0 = 1;
        USER_IO1 = 0;
        USER_IO2 = 0;
        TxBuffer[TxData++] = SUCCESS;
        break;
    case DATA_TWO:
        ConsolePutROMString( (ROM char *)" Received TWO.\r\n" );
        USER_IO0 = 0;
        USER_IO1 = 1;
        USER_IO2 = 0;
        TxBuffer[TxData++] = SUCCESS;
        break;
```

Figure 3.6. RFD Node Receiving 3-Bits That Represent 8 Levels

3.4 Conclusion

Using the Zigbee protocol and the Microchip ICDEM Z kit. We provided a reliable low power wireless control for the Magnetic Force Actuator. Three bits represent eight different force levels which can be inputted or preprogrammed on a Controller and then sent wirelessly to a network of Magnetic Force Actuating nodes, where each node will perform the command it receives irrespectively and regardless of the other nodes in the network.

CHAPTER 4

Atomic Force Microscope

4.1 Introduction

Atomic Force Microscopy was invented in 1986, which was based on Scanning Tunneling Microscopy 1981. AFM gives us the ability to get high resolution images of surfaces (down to the nano scale). It can display features as small as an atomic lattice. With this high resolution, scientists can even come closer to the atom more than what they would have ever thought. AFM has three major components: a laser beam, a photodetector, and a cantilever. The basic operation of an AFM is as follows:

- The cantilever which has a tiny tip (probe) approaches a surface to be scanned.
- A laser beam will be directed on the cantilever's back surface while it is moving over the surface.
- The tiny tip interacts with the atoms on the surface causing the cantilever to deflect upward or downward and that results in a change in the laser beam reflection angle.
- The photodetector records the change in reflected laser beam and relates it with the deflection as seen in figure 4.1.

The recorded results can be represented as a surface topography image with a very high resolution. However, imaging the surface is not the only application AFM can

be used in, other useful calculations can be acquired from the interaction between the surface and the tip. For example, if the surface and the tip had magnetic properties then a relation can be established between them to represent the attraction/repulsion forces.

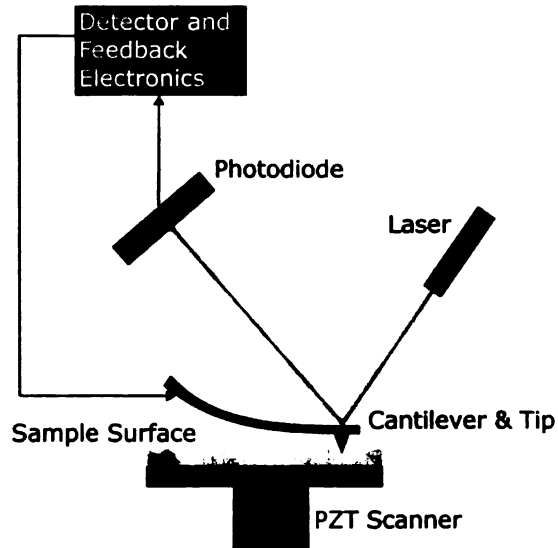


Figure 4.1. Atomic Force Microscope [3]

There are two different types of imaging modes in AFM, static (contact) mode and dynamic (non-contact) mode. In the static mode, the controller inside the AFM tries to keep the force between the tip and the surface constant by adjusting the the Z axis (the distance between the tip and the surface), so, the change in the Z axis will be recorded and analyzed. In the dynamic mode the cantilever will be oscillating far away from the surface at a certain resonance frequency. Therefore, the amplitude of oscillation, phase and frequency are monitored by the AFM for any changes which then describes interaction between the tip and the surface.

4.2 Magnetic Force Measurements

4.2.1 Introduction

To be able to record the output of the Magnetic Force Actuators discussed in the previous chapters, we have decided to use AFM because it is better than other technologies [20] as listed in the following table 4.1:

Table 4.1. Comparison Between AFM and Other Technologies

	AFM	TEM	SEM	Optical
Max resolution	Atomic	Atomic	1s nm	100s nm
Typical cost (x \$1,000)	100 - 200	500+	200 - 400	10 - 50
Imaging Environment	air, fluid, vacuum, special gas	vacuum	vacuum	air, fluid
In-situ	Yes	No	No	Yes
In fluid	Yes	No	No	Yes
Sample preparation	Easy	Difficult	Easy	Easy

We used the basic Nanosurf EasyScan 2 AFM[21] which provides static (contact) mode. Utilizing the features in the static mode and using it along with a magnetized cantilever tip, we were able to analyze some properties of the Magnetic Force Actuator, which are discussed in the next sections. The normal operation of the static mode requires the tip to “touch” the surface, however, in this application (using the magnetized tip) approaching the tip close to the surface will damage it. Consequently, We decided to use the static mode in a special way which will be explained later.

4.2.2 Measurements

The setup for this measurement required the use of all three components of this thesis; the fabricated chip, the wireless control, and AFM. The Fabricated chip was placed under the AFM scan head, however, the packaging of the chip made this step difficult. Because the chip could not easily fit under the scanning head special mounting tools and wiring were designed to allow the scan head to move freely on top of the MFA.

Once the chip was installed under the scanning head, it was tested to make sure it is functional. The test involved using the Controller to send certain commands and observe the current consumption increases when a higher power was requested. Also, another test was to make sure that the output frequency matches the desired one. After securing that, the circuit was turned off. A magnetically doped cantilever was then magnetized using a strong magnet, then it was installed on the scanning head. The next step is to switch on the MFA and send it a 111 input using the manual user input mode on the Controller. By doing so, we make sure that the tip will not collapse into the chip because the scan head controller will notify us as soon as there is an interaction between the two, thus, by setting on maximum force level we will be able to detect such interaction early on.

Using the naked eye by looking through the magnifier on the scanning head, the cantilever is brought closer to the chip by moving the leveling the screws downwards. It is important to keep the head leveled to get accurate measurements. After the manual approach by using screws is completed, an automated approach using the Z controller in the software of the EasyScan2 is applied. The Z controller is a standard PID controller to keep the tip at a certain distance from the chip. The distance between the tip and the chip is represented as “Set Force = 20nN” which means that the tip will come closer to the surface (in the Z direction) until it detects a force with a magnitude of 20nN.

Once the automatic approach is done and the tip is at a reference point $Z = Z_0$ (where the force exerted is 20nN+, we freeze the Z controller, so, it does not move the cantilever anymore. By freezing the Z controller we guarantee that the cantilever remains at the same position (Z_0) in all experiments. Now since we used the maximum possible force generated by the MFA, we will not be able to detect the smallest forces. Therefore, the tip is brought closer to the sample while keeping a safe range between the tip and surface. The reference point now is $Z = Z_1$ and this will be the final Z

which we will use in all measurements. The Z controller is still frozen, we just brought the tip closer so we can detect smaller forces for the next measurements.

Figure 4.2 shows the first spectroscopy measurement when the user input is 111, it should produce the largest force on the tip. There are 256 data points during this measurement, each data point is an average of 8 samples which were taking separately. There was a five second period between each sample. So, in total this measurement took 40 seconds to complete, therefore, it contains 2048 measurements. All these points were averaged. Therefore, the total average deflection for user input 111 is $5.21523 \times 10^{-08} \text{m}$.

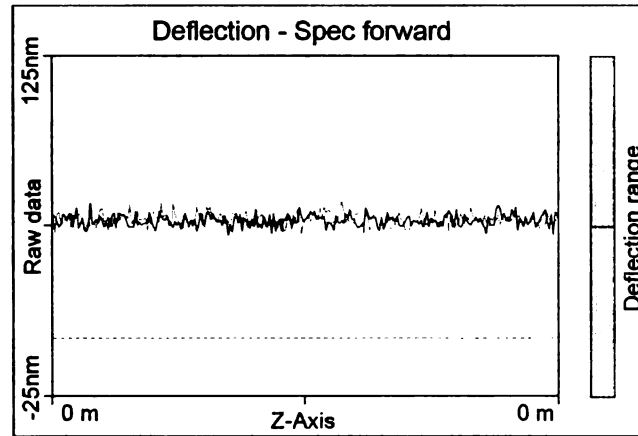


Figure 4.2. Tip Deflection at 111

While keeping the same reference Z value (keeping the tip at a distance $Z = Z_1$) the user input will be changed to 110 and the deflection will be recorded again. The same method is used 256 points with 8 averages and five seconds in between. The deflection produced for user input 110 is $4.91725 \times 10^{-08} \text{m}$ and shown in figure 4.2. The same measurements are carried for the rest of the levels 101,100,011,010,001, 000, and finally when the chip is switched off. The final results as shown in table 4.2 and figure 4.4. .

The spring constant K for the magnetic cantilever was provided as a range between 1 to 5 from the manufacturer [22], so, we will represent the corresponding forces as a

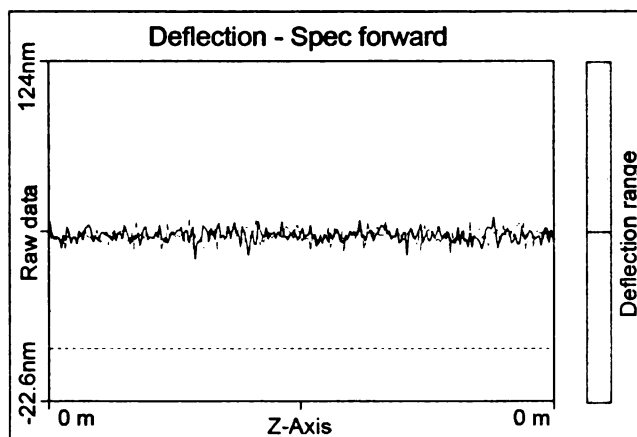


Figure 4.3. Tip Deflection at 110

Table 4.2. Different User Inputs with their Corresponding Deflections

User Input	Tip Deflection
OFF	2.41301E-10
000	2.79E-08
001	3.29E-08
010	3.73E-08
011	4.00E-08
100	4.44015E-08
101	4.79164E-08
110	4.91725E-08
111	5.21523E-08

range as well. The actual K will be sent to us in the near future. Table 4.3 shows three possible values of K and their corresponding force. A graph of that is shown in figure 4.5.

As previously discussed and shown in figure 2.17, the current generated by the Class E PA will be running at 900MHz, it will cause the actuator to produce a changing (alternating) magnetic field at that frequency. However, the cantilever's resonance frequency is only 60KHz so the cantilever itself won't be able to achieve and oscillate at such high frequencies, so, it will act as a filter giving us an average RMS value. Therefore, the results we are seeing in table 4.5 represent the averaged force after being filtered out by the cantilever.

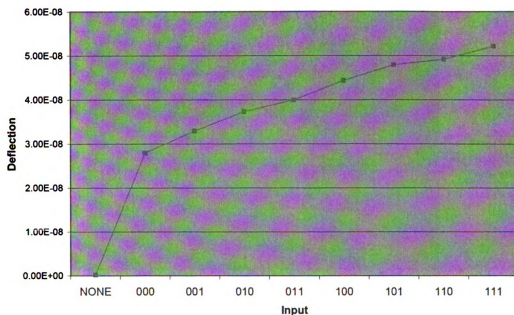


Figure 4.4. Tip Deflection at All Input Levels

Table 4.3. Different User Inputs with their Corresponding Forces

Input	Force at K=1	Force at K=3.0	Force2 at K=5
OFF	2.41E-10	6.03252E-10	1.2065E-09
000	2.79E-08	8.38E-08E-10	1.40E-07
001	3.29E-08	8.23E-08	1.65E-07
010	3.73E-08	1.12E-07	1.87E-07
011	4.00E-08	1.20E-07	2.00E-07
100	4.44E-08	1.33E-07	2.22E-07
101	4.79E-08	1.44E-07	2.40E-07
110	4.92E-08	1.48E-07	2.46E-07
111	5.22E-08	1.56E-07	2.61E-07

4.2.3 Conclusion

Using the AFM technology, we were able to compute the force actuated from the MFA at a certain distance in the Z direction. A Magnetically doped cantilever was used and placed on top of the 20pH inductor, for an example see figure 4.6. Arrow 1 points at the base of the cantilever. Arrow 2 points at the cantilever itself. Note that the cantilever is actually covering the small 20pH inductor beneath it. The range of the force generated out of the MFA, at the same Z distance, is from $2.41 \times 10^{-10} \text{N}$ to $5.22 \times 10^{-08} \text{N}$ with a cantilever spring constant $K=1$ and $1.40 \times 10^{-9} \text{N}$ to $2.61 \times 10^{-07} \text{N}$

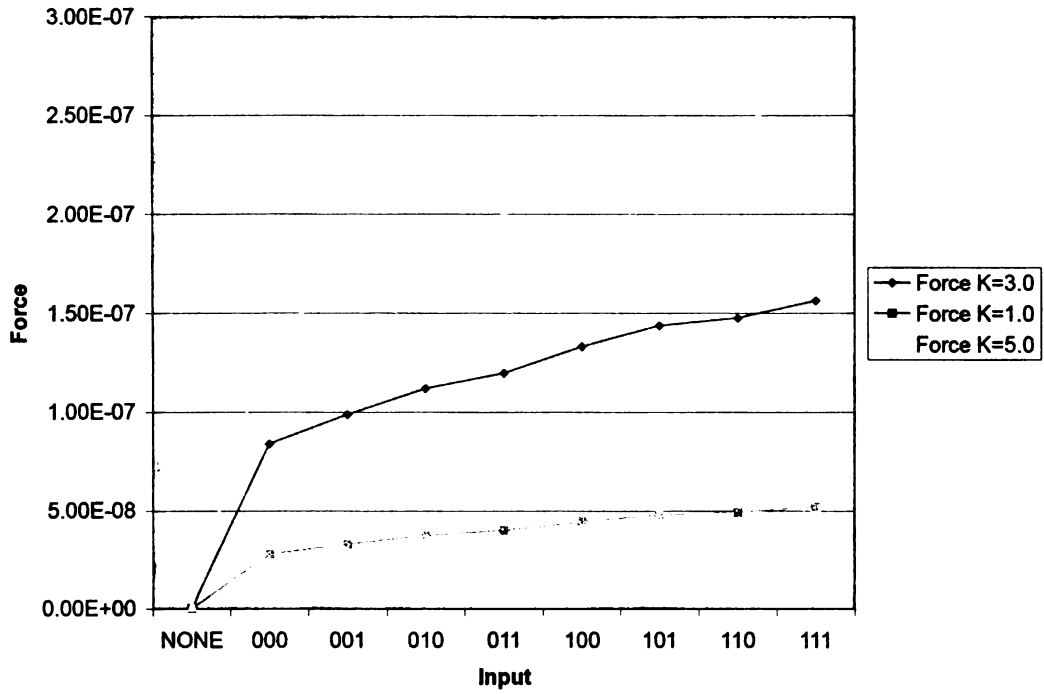


Figure 4.5. Force Exerted On Tip at All Input Levels At Distance Z1

with a cantilever spring constant $K=5$.

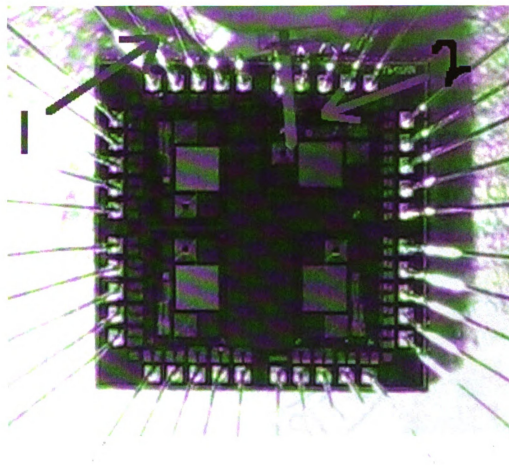


Figure 4.6. Magnetic Cantilever on Top Of MFA

CHAPTER 5

Conclusions

5.1 Results

We were able to design, simulate, and test a wirelessly controlled magnetic force actuator as illustrated in figure 5.1(a) and 5.1(b).

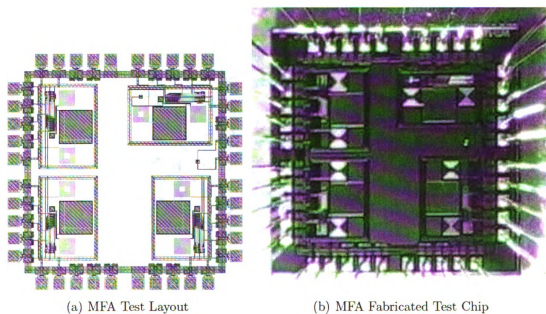


Figure 5.1. Magnetic Force Actuator Chip

It can produce eight different levels of magnetic forces as shown in figure 5.2. These forces were measured using a magnetically doped cantilever shown in figure 5.3

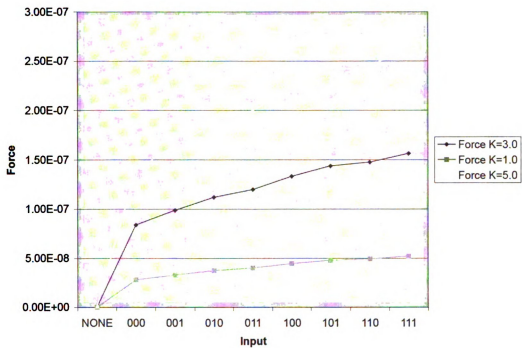


Figure 5.2. Force Exerted On Tip at All Input Levels At Distance Z1

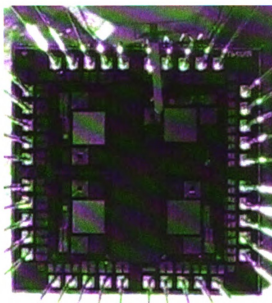


Figure 5.3. Magnetic Cantilever on Top Of MFA

The overall work can be summarized in the following figure 5.4. A wireless network of Magnetic Force Actuators which can be controlled using a Controller (Coordinator)

to produce eight different output levels using a preprogrammed algorithm or a manual user input.

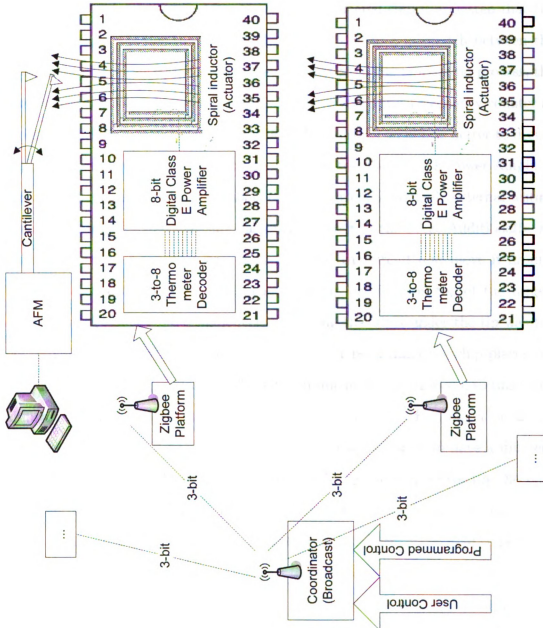


Figure 5.4. Thesis Block Diagram

5.2 Future Work

For future development it would be desired to have a more precise model for on-chip inductors and capacitors. After testing the fabricated chip it appeared that the output frequency was not tuned correctly. This is due to a mismatch between the values used in the simulations and the result values from the fabrication process, the desired frequency was supposed to be 900MHz however, using a frequency counter at the output pin; the tested frequency was 600MHz. Also, It would be better to design on-chip test components to be able to measure and test the Class E Power Amplifier internally instead of using external tools because currently available external testing devices could not precisely measure the output power of the PAE. Additionally, an AFM scanner with a movable base that can hold the circuit and move it around is needed because it would place the cantilever tip precisely on top of the target, instead of using manual hand maneuvers. Locating the 20pH under the tip was the most difficult part: first, the packaging process after fabricating the chip places the bonding wires upwards (coming out of the pad frame in the Z direction), so this made it difficult for the cantilever to reach the surface of the chip, which might break the bond wires or the cantilever itself, therefore, it would be better to have a different type of packaging which places the bond wires on the sides instead of the top. Second, the current method used to place the tip exactly on top of the $6\mu\times 6\mu$ uses the naked eye as a guide, consequently other more accurate methods should be used to precisely place the tip. Because of these two reasons it was difficult to repeat the measurements and get the same exact values of the force for different setups. As a result, future work should have a different layout and packaging to easily locate and scan the actuator.

APPENDIX A

Magnetic Force Actuator Test Chip

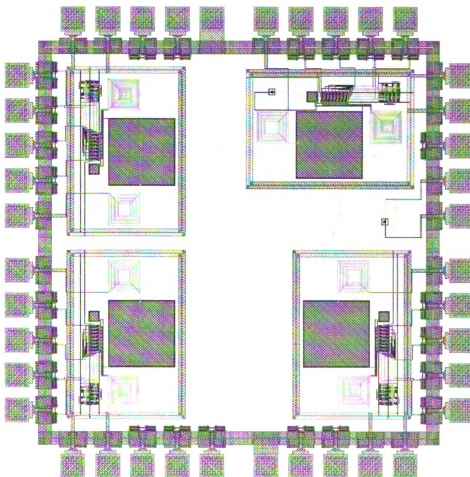


Figure A.1. MFA Test Chip Layout

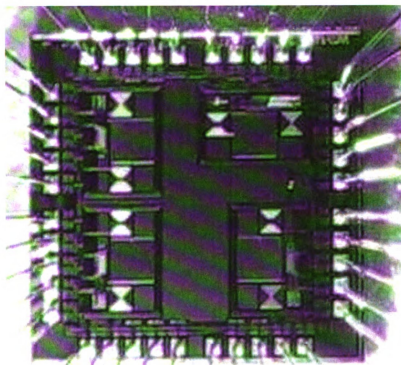


Figure A.2. MFA Fabricated Test Chip

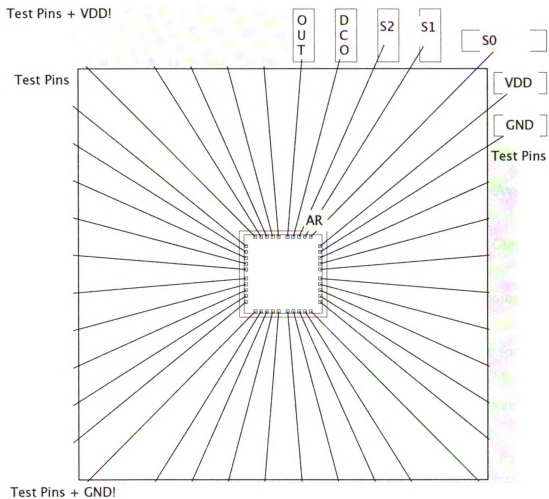


Figure A.3. MFA Pin Diagram

BIBLIOGRAPHY

- [1] N. O. Sokal and A. D. Sokal, "Class E - A new class of high-efficiency tuned single-ended switching power amplifiers," *IEEE Journal of Solid-State Circuits*, vol. 10, pp. 167–176, Jun. 1975.
- [2] Microchip. (2007, May) Zigbee stack. [Online]. Available: <http://www.microchip.com/zigbee/>
- [3] Wikipedia. (2007, May) Atomic force microscope. [Online]. Available: <http://en.wikipedia.org/wiki/AFM>
- [4] J. M. Rabaey, A. Chandrakasan, and B. Nikolic, *Digital Integrated Circuits A Design Perspective*. Prentice-Hall, 2006.
- [5] S. J. Ball, C. Folsom, and A. B. McLean, "A compact nano-positioning stage with high vibrational eigenfrequencies," 2005.
- [6] H. Liu, B. Lu, Y. Ding, Y. Tang, and D. Li, "A motor-piezo actuator for nano-scale positioning based on dual servo loop and nonlinearity compensation," 2003.
- [7] MOSIS. (2007, May) Ncsu cdk. [Online]. Available: <http://www.mosis.org/products/fab/vendors/amis/c5/>
- [8] F. T. Abu-Nimeh and F. M. Salem, "Digital class e power amplifier for the rf band," Proceedings of the IEEE International Conference on Mechatronics and Automation (ICMA '06), 2006.
- [9] B. Razavi, *RF Microelectronics*, 1st ed. Upper Saddle River, NJ, USA: Prentice-Hall, Inc., 1997.
- [10] S. C. Cripps, *RF Power Amplifiers for Wireless Communications*, 2nd ed. Norwood, MA, USA: Artech House, Inc., 2006.
- [11] T. H. Lee, *The Design of CMOS Radio-Frequency Integrated Circuits*, 2nd ed. Cambridge University Press, 2003.
- [12] A. M. Niknejad. (2007, May) Asitic. [Online]. Available: <http://rfic.eecs.berkeley.edu/~niknejad/asitic.html>

- [13] D. K. Choi and S. I. Long, "High efficiency class e amplifiers for mobile and base station applications."
- [14] P. Alinikula, K. Choi, and S. I. Long, "Design of class e power amplifier with nonlinear parasitic output capacitance," *Circuits and Systems II: Analog and Digital Signal Processing*, IEEE Transactions, 1999.
- [15] P. Cruise, C.-M. Hung, R. B. Staszewski, O. Eliezer, S. Rezeq, K. Maggio, and D. Leipold, "A digital-to-rf-amplitude converter for gsm/gprs/edge in 90-nm digital cmos," 2005.
- [16] O. S. University. (2007, May) Osu standard cell library. [Online]. Available: <http://vcag.ecen.okstate.edu/projects/scells/>
- [17] N. C. S. University. (2007, May) Ncsu cdk. [Online]. Available: <http://www.eda.ncsu.edu/>
- [18] HyperPhysics. (2007, May) Solenoid magnetic field calculation. [Online]. Available: <http://hyperphysics.phy-astr.gsu.edu/hbase/magnetic/solenoid.html>
- [19] hasse.nl. (2007, May) A technical overview of wireless technology. [Online]. Available: <http://zigbee.hasse.nl/>
- [20] Agilent. (2007, May) What is atomic force microscope. [Online]. Available: http://www.molec.com/what_is_afm.html
- [21] Nanosurf. (2007, May) Nanosurf eastscan2. [Online]. Available: <http://www.nanoscience.com/products/easyScan2.html>
- [22] AppNano. (2007, May) Magt data sheet for magnetic force microscopy probes. [Online]. Available: http://www.appnano.com/pdf/Datasheet_MAGT.pdf

MICHIGAN STATE UNIVERSITY LIBRARIES



3 1293 02956 1788